Chapter II: Geochronology techniques

1. Introduction: General principles of geochronology

Different geochronological techniques were utilized during this study to constrain the ages of the basement, the deposition of the Katangan sequence and the thermal events that affected this sedimentary sequence. Therefore, one complete chapter is devoted to the general principles of geochronology and to the detailed description of the different techniques that were used.

Radioisotope geochronology is based on the law of natural disintegration of elements. In nature, some elements comprise different isotopes. Isotopes are atoms of the same chemical element with the same atomic number but with different mass numbers (they differ in the number of neutrons) (Faure, 1986). Some of these isotopes are radioactive, meaning that their nuclei are unstable and able to spontaneously break down (decay) to stable isotopes of different elements. This process ends when the newly formed isotope is stable (Williams, 1998). Each isotope decays at a specific rate (represented by the constant λ) that is independent of pressure, temperature, chemical state, …

Radioactive decay can be described by the equation (Williams, 1998):

$$D = P\,(1-e^{-\lambda t}) \qquad (1)$$

Where:

D = the number of daughter atoms created

P = number of parent atoms, provided that no daughter atoms were present initially and provided that no parent or daughter atoms were either added to or lost from the system since t was equal to zero.

λ = the decay constant for the isotope concerned, representing the probability that an atom will decay within a stated unit of time.

t = period of time

From the decay constant of a given radioactive atom, the half-life of this atom may be calculated. This is the time required for one half of the given radionuclide to decay and is provided by:

$$T_{1/2} = \ln 2/\lambda \qquad (2)$$

Where:

$T_{1/2}$ = half life of the isotope

λ = decay constant

Table 1 shows some of the radioactive isotopes commonly used in geochronology as well as their daughter isotopes and ½ lives.

Parent isotope	Daughter product	Half life (years)	λ (yr^{-1})
^{40}K	^{40}Ar	1.25×10^{9}	4.962×10^{-10}
^{87}Rb	^{87}Sr	48.8×10^{9}	1.42×10^{-11}
^{147}Sm	^{143}Nd	106.0×10^{9}	6.54×10^{-12}
^{232}Th	^{208}Pb	14.01×10^{9}	4.9475×10^{-11}
^{235}U	^{207}Pb	0.704×10^{9}	9.8485×10^{-10}
^{238}U	^{206}Pb	4.468×10^{9}	1.55125×10^{-10}

Table 1: Some radioactive elements with their decay constants and their half-lives. After Steiger (1977) and Faure (1986)

2. Choice of techniques

The initial considerations for constraining the age of the deposition of the Katangan sequence involved a selection of isotopic techniques such as Rb–

Sr, Pb–Pb, U- Pb, Ar-Ar and Sm-Nd. However, after fieldwork and detailed petrography had been carried out, it became apparent that some of these methods would not be suited for the purpose of this thesis. The different lithologies have been reworked and the rocks are very altered. Use of Rb-Sr systematics, for example, would not have allowed us to constrain the age of the deposition, but rather the age of the latest reworking event. It was decided that Sensitive High Resolution Ion Microprobe (SHRIMP) U-Pb dating would be undertaken to analyse detrital, xenocrystic and magmatic zircons from the Katangan Sequence and the basement, as well as some metamorphic monazites from the sedimentary sequence. Magmatic zircons provide information on the time of emplacement of granitoids and extrusive rocks. The analysis of detrital zircons provides the maximum age of sedimentary deposition and information on the source or the sources of these sediments, whereas analyses of metamorphic monazites provide constraints on the timing of metamorphism. To supplement the data on metamorphism, some Ar-Ar dating was undertaken on biotite, sericite and K-feldspar. These last data provide age constraints on the metamorphic events but also information on the cooling history and thermal disturbances undergone by the samples. Ar-Ar was also used on detrital muscovite to provide the maximum age of the sedimentary rocks from which it was extracted. The two techniques U-Pb and ^{40}Ar-^{39}Ar used in this work are described in detail in the following sections.

3. The U-Pb dating technique

a. Principles of the method

This technique is based on three of the isotopes of uranium and thorium, all of which decay to different isotopes of lead. Uranium, atomic number 92, includes 11 isotopes, of which three are radioactive: ^{235}U, ^{238}U and ^{234}U. Thorium, atomic number 90, has only one radioactive isotope: ^{232}Th. The

decay paths of ^{232}Th, ^{238}U and ^{235}U to the stable isotopes ^{208}Pb, ^{206}Pb, ^{207}Pb, respectively, are shown in Figures 1a, b and c. Lead (Z=82) includes four natural isotopes, ^{204}Pb, ^{206}Pb, ^{207}Pb, ^{208}Pb, of which ^{204}Pb is produced by nucleosynthesis.

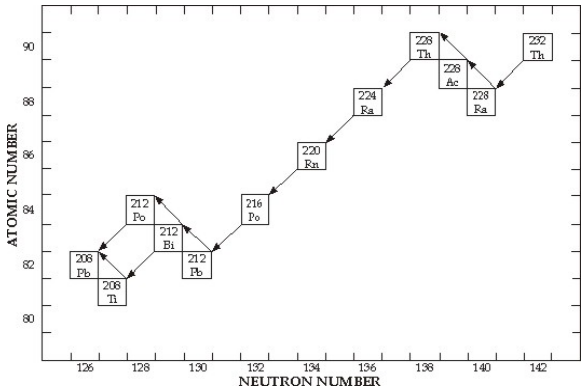

Figure 1a: The decay of ^{232}Th to ^{208}Pb (from Faure, 1986)

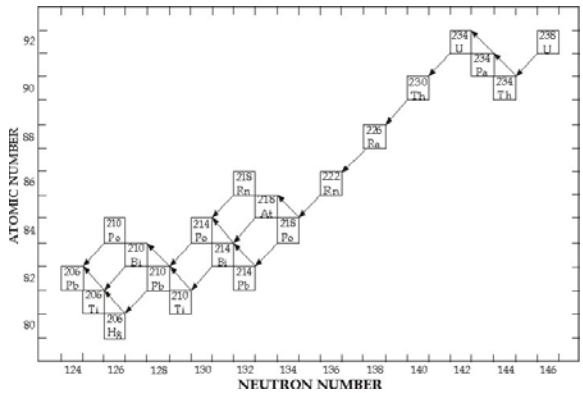

Figure 1b: The decay of ^{238}U to ^{206}Pb (from Faure, 1986)

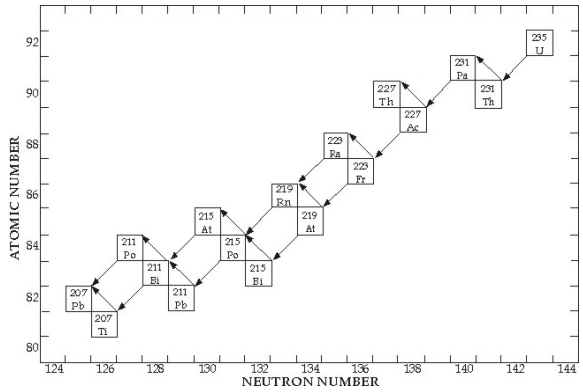

Figure 1c: The decay of ^{235}U to ^{207}Pb (from Faure, 1986)

As seen above, the two uranium isotopes decay to two isotopes of lead. In an ideal case with a system rich in uranium but lacking any initial lead, two equations can be written. The decay of ^{238}U to ^{206}Pb as a function of time is described by:

$$^{206}Pb/^{238}U = (e^{\lambda_{238}T}-1) \quad (3)$$

and the decay of ^{235}U to ^{207}Pb is described by:

$$^{207}Pb/^{235}U = (e^{\lambda_{235}T}-1) \quad (4)$$

b. U-Pb SHRIMP dating

This section is a brief and simplified summary of the U-Pb SHRIMP dating technique. When not mentioned the sources are Williams (1998) and Ireland (1995).

SHRIMP systematics: A schematic layout of of SHRIMP II is presented in figure 2. The basic principle of an ion microprobe is to focus a fine primary oxygen ion beam on a solid target (sample) in order to generate a secondary ion beam by eroding or "sputtering" the sample, and by ejecting particles from the surface of the sample. In the primary column, negative oxygen ions are produced by acceleration through 10 kV under high vacuum. Sputtering occurs and a fraction of the ejected particles is ionised and electrostatically removed from the sample. This secondary ion beam goes through the electrostatic analyser and the magnet where the ions are separated according to charges and masses. Eight different ions and molecules (Zr_2O, ^{204}Pb, ^{206}Pb, ^{207}Pb, ^{208}Pb, ^{238}U, ThO, UO) and the background are counted on a single collector in peak switching mode. Data for this study were acquired on SHRIMP I and II. The lower limit for the sample spot size for SHRIMP I is 15μm while it is ~ 5 μm for SHRIMP II (Williams, 1998).

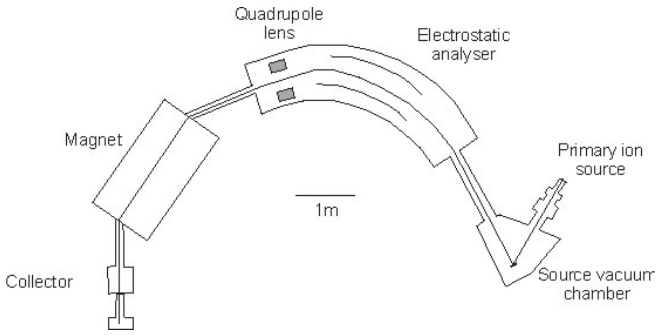

Figure 2: Schematic layout of SHRIMP II at the RSES-ANU (Canberra) (from Williams, 1998)

Standardization: In the SHRIMP, isotopic mass fractionation produced during the sputtering and interference of hybrids on the Pb peaks is corrected by normalising the measured ratios to a standard zircon. In zircon analysed by SHRIMP, a correlation between $^{206}Pb/U^{+}$ and UO^{+}/U^{+} exists (Compston et al., 1984; Williams and Claesson, 1987). The daily calibration with the standard zircon consists of defining the curve that relates these two ratios. The analyses obtained in this study were undertaken with reference to the two standards used at the Research School of Earth Sciences (R.S.E.S.), Australian National University (A.N.U.), Canberra, Australia. A Duluth Complex zircon, AS3, dated at 1999.1 Ma with a $^{206}Pb/^{238}U$ = 0.1859, was utilised to reference the U/Pb ratios; the Sri Lankan zircon, SL13, dated at 572 Ma with $^{206}Pb/^{238}U$ = 0.0928, was used to determine the U and Th concentrations.

The criteria to select a good quality U-Pb standard are as follows.

- The composition and the crystallinity must be close to that of the mineral analysed.
- It must be mineralogically pure.
- The quantity of grains must be sufficient enough to be able to provide material for a large number of analyses (several thousands of SIMS analyses and several TIMS calibration analyses).
- The diameter of the grains must be greater than 50 μm.
- The Pb/U and Pb/Th ratios must be uniform and concordant throughout.

- The age of the standard must be old enough to include sufficient radiogenic lead, but not too old to produce radiation damage.

Sample preparation: In a first step, rocks are reduced in a jaw crusher down to millimetric chips. The chips are then inserted in a pulverizer to produce a powder with a grain size less than 250 μm. The powder is then put on a Wilfley table, which makes a first separation between heavy and light fractions. The end of the separation is undertaken using the Franz magnetic separator and heavy liquids (Bromoform and Iodine-methane). The last stage is to hand-pick zircons and monazites under a binocular microscope. Zircons and monazites are randomly selected without preference to colour, shape, inclusions or alteration. In the case of magmatic rocks, all the zircons are taken. For the sedimentary rocks, only a fraction of the total amount of zircons is taken but the same conditions of selection apply. Zircons from the sample, as well as standard zircons, are mounted onto the surface of an epoxy disc and polished.

Cathodoluminescence: After being mounted onto the surface of an epoxy disc, cathodoluminescence images of zircons and monazites are taken using a Scanning Electron Microscope. The principle of cathodoluminescence imaging is as follows. Minerals are stimulated by an electron beam and react by emitting X-rays, secondary electrons, backscattered electrons and Auger electrons (Hayward, 1998). In the case of zircons, the dark areas are related to U-enriched zones whereas the very clear areas are a sign of relative depletion in uranium. It is not possible to get images from the monazites as they come out completely black.

c. Data acquisition and statistic treatment of the data

Instrumental conditions and data acquisition were as described by Compston et al. (1984; 1992). For each spot, data were collected in sets of six or seven scans through the mass range as in Compston et al. (1984;

1992). Data were statistically treated according to Compston et al., (1992) with a software developed at the RSES. Radiogenic ratios of single data points are shown in tables and are given with one-sigma errors. The mean age of a population is calculated as weighted mean and is given with a 95% confidence level.

d. Evaluation of the data

The common lead measured during a SHRIMP analysis is a mixture of lead comprising the contaminating lead burned off from the mount surface and the conductive gold coat, and the non-radiogenic or initial Pb incorporated by the mineral. The amount of common Pb correction is conventionally given by the notation f, which is the fraction of the total ^{206}Pb that is common ^{206}Pb. There are three methods used for the calculation of common Pb in ion microprobe U-Pb zircon analyses:

- The ^{204}Pb correction: all ^{204}Pb is unradiogenic and this correction uses the directly measured ^{204}Pb isotope abundance. The isotopic composition of the common Pb is assumed to approximate a model composition (Stacey and Kramers, 1975) consistent with the age of the zircon. As the ^{204}Pb peak is relatively very small, measurements have poor precision, but this method does have fewer assumptions than the other methods.
- The ^{207}Pb correction: this is primarily used for young (e.g. Phanerozoic) samples where the emphasis is on obtaining accurate $^{206*}Pb/^{238}U$ ages, rather than $^{207*}Pb/^{206*}Pb$ data. If the approximate age of the sample is known, and the sample is assumed to be concordant, then the fraction of common Pb can be calculated from the measured (total) $^{207}Pb/^{206}Pb$ and the assumed $^{207}Pb^{206}Pb$ composition.
- The ^{208}Pb correction: this correction is based on the measured $^{208}Pb/^{206}Pb$ and $^{232}Th/^{238}U$ ratios, and assumes that the Th/U has remained closed or undisturbed in the spot analysed. The expected radiogenic $^{208*}Pb/^{206*}Pb$ can be calculated from the measured $^{232}Th/^{238}U$

in the zircons, and the assumed age and common $^{208}Pb/^{206}Pb$ composition (Compston et al., 1984). Any deviation from the expected value is assumed to be due to common Pb. This method is particularly suitable for zircons with low Th (and very low Th/U).

e. Data presentation

The conventional "Wetherill" Concordia diagram: From equations (3) and (4), Wetherill's (1956) work led to the definition of a curve, in a plot of the $^{207}Pb/^{235}U$ vs $^{206}Pb/^{238}U$ which defines the evolution of these ratios as a function of time. This reference curve where the two ratios give the same age and which shows the change in those ratios as a function of time is called the Concordia (Figure 3).

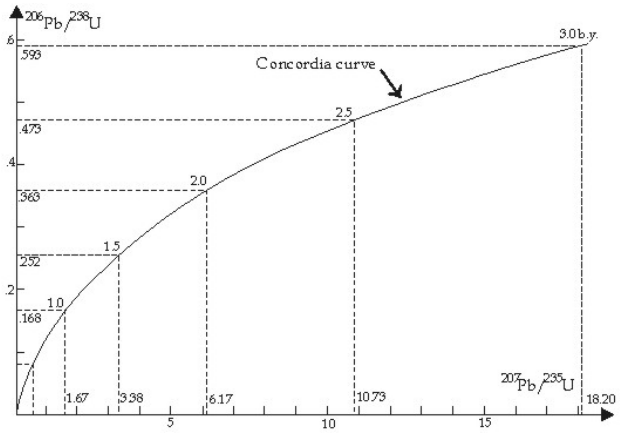

Figure 3: Conventional concordia diagram (after Wetherill, 1956)

The "Tera-Wasserburg" Concordia diagram: Described and revised by Tera and Wasserburg (1972), this diagram shows the parent/daughter ratio ($^{238}U/^{206}Pb$) plotted on the "x" axis and the Pb isotopic ratio ($^{207}Pb/^{206}Pb$) on the "y" axis (Figure 4).

The Tera – Wasserburg diagram has three advantages over the Wetherill plot (Wiliams, 1998):

- The $^{207}Pb/^{235}U$ ratio is not calculated, and the data are plotted as measured.
- Regression analysis of data is made easier because errors in measuring $^{207}Pb/^{206}Pb$ and $^{238}U/^{206}Pb$ are much more weakly correlated than those in measuring $^{207}Pb/^{235}U$ and $^{206}Pb/^{238}U$.
- The initial Pb isotopic composition can be found at the intersection between the $^{207}Pb/^{206}Pb$ axis and the mixing line defined by a plot of analyses uncorrected by the initial Pb.

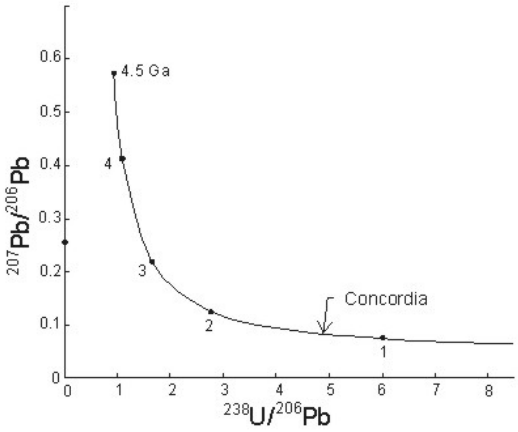

Figure 4: Tera Wasserburg concordia diagram (1972)

4. ^{40}Ar-^{39}Ar dating technique

a. Principles of the method

This method is an improvement of the K-Ar method, which uses the decay of potassium to argon. In nature, potassium has three isotopes in constant proportions, ^{41}K, ^{40}K, ^{39}K, where only ^{40}K is radioactive. ^{40}K disintegrates to ^{40}Ca (in 89% of the decays) and to radioactive ^{40}Ar (in 11% of the decays). Applied to the K-Ar system, the equation giving the age of the system becomes:

$$T = 1/\lambda \ln(1 + (\lambda/\lambda_\varepsilon).(^{40}Ar^*/^{40}K)) \quad (5)$$

Where

$^{40}Ar^*$ is radioactive Ar

$\lambda = \lambda_\varepsilon + \lambda_\beta = 5.5543.10^{-10}\ y^{-1}$

$\lambda\varepsilon = 0.581.10^{-10}\ y^{-1}$

$\lambda_\beta = 4.962.10^{-10}\ y^{-1}$

This method of dating has a major disadvantage because two types of analytical techniques are needed. Potassium must be measured by chemical techniques, while argon must be measured by gas source mass spectrometry. With this method, the results cannot be applied easily to decipher polyphase geological contexts and in many cases the results are only apparent ages.

These problems are overcome by irradiation of the samples. In the presence of a neutron flux, ^{39}K transforms to ^{39}Ar. Merrihue (1965), Merrihue and Turner (1966) and Mitchell (1968) described and rigorously established the principles of the ^{40}Ar-^{39}Ar technique. The first dating was done on meteoritic samples (Turner, 1966). Since then, numerous ages have been obtained on terrestrial samples.

The sample to be dated is irradiated in a nuclear reactor. The reaction ^{39}K (n, p) → ^{39}Ar is activated by a fast neutron flux. At the same time, interfering argon, potassium, chlorine and calcium isotopes are created. The reaction is not total but its yield can be calculated. The following equation gives the amount of ^{39}Ar created from ^{39}K after neutron irradiation:

$$^{39}Ar = {}^{39}K\ \Delta T \int \phi(\varepsilon)\ \tau(\varepsilon)\ \delta(\varepsilon) \quad (6)$$

Where

ΔT = length of the irradiation

$\phi(\varepsilon)$ = neutron flux density at energy ε

$\tau(\varepsilon)$ = capture cross section of ^{39}K for neutrons of energy ε

The ratio $^{40}Ar^*/^{39}Ar$ is obtained after correction of the measured mass 40 for the atmospheric contribution (assuming that the atmospheric $^{40}Ar/^{36}Ar$ ratio is 295.5 and has remained relatively constant through geological time) and after correction for isotopes created during irradiation (i. e. Ar, K, Cl, Ca, with masses 36 to 40). During irradiation, some argon isotopes appear, created by interactions between neutrons and K, Ca, Cl and Ar isotopes. These newly created isotopes remain in negligible proportions. After irradiation of a sample, its $^{40}Ar/^{39}Ar$ is given by:

$$^{*40}Ar/^{39}Ar = {}^{40}K/^{39}K \,.(\lambda_\varepsilon/(\lambda_{\varepsilon+}\lambda_\beta)) \,.\, (e^{(\lambda\varepsilon+\lambda\beta)}-1)/\,(\Delta T+\phi(\varepsilon)\,\tau(\varepsilon)\,d(\varepsilon)) \qquad (7)$$

Merrihue (1965) suggested the addition of a sample of known age (T_s) to the irradiated sample. This standard allows the definition of a J quantity, valid for all the unknown age samples (t), for the considered irradiation.

$$J = (e^{(\lambda\varepsilon+\lambda\beta)Ts}-1) \,/\, (^{40}Ar/^{39}Ar)_s \qquad (8)$$

With J, the final chronometric equation can be written and is valid for all the unknown age samples irradiated with the standard:

$$t = -1\,/\lambda \ln\,(1+((^{40}Ar\,/^{39}Ar)\,.\,e^{\lambda ts}-1)\,/\,(^{40}Ar\,/^{39}Ar)_s) \qquad (9)$$

b. Ar-Ar mass spectrometry

Concept of isotopic closure temperature in minerals: The closure or blocking temperature is related to the point in time when a mineral crosses a thermal threshold, below which it behaves as a closed system (Figure 5). Above this closure temperature, daughter isotopes produced inside the system diffuse outwards to establish equilibrium with the local environment.

In contrast, below this temperature, daughter isotopes accumulate in the system, or mineral. Dodson (1973) developed a theory where it is shown that this closure temperature Tc is dependent on several parameters. For thermally activated diffusion ($D=D_0e^{-E/RT}$) it is given by:

$$T_C = R/[E \ln (A \tau D_0/a^2)] \quad (10)$$

Where:

T_C = closure temperature

R = gas constant

E = activation energy

τ = time constant with which the diffusion coefficient D diminishes

a = characteristic diffusion size

A = numerical constant depending on geometry and decay constant of parent.

For slow cooling, the passage between open and closed system is progressive. During this time period, the system behaves as a partly open system in which a progressively greater proportion of radiogenic isotopes remains in the system until complete retentivity is reached. On the other hand, for fast cooling, the passage is quasi-instantaneous. Therefore, Tc is higher for a mineral subjected to a rapid cooling than it is for one subjected to slow cooling. Furthermore, the size of the grain, its chemistry and its crystalline structure will influence Tc. Hence, for a same mineral, closure temperature variations can be noted (Table 2).

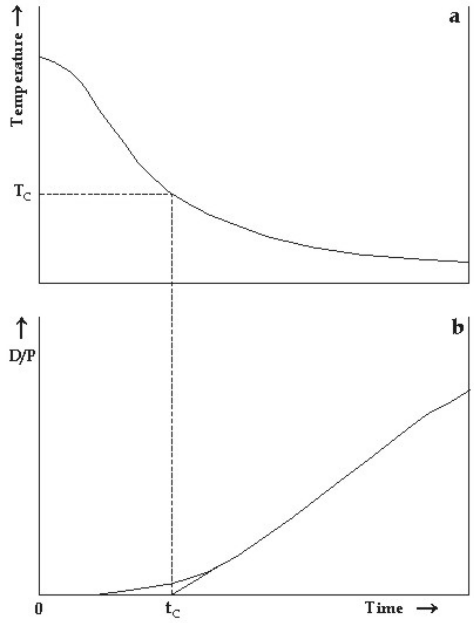

Figure 5: Definition of closure temperature; a- cooling curve; b- accumulation curve. D/P daughter/parent ratio. Fine broken lines show approximate limits of transitional time-temperature range (after Dodson, 1973).

Mineral	Temperature	Reference
Muscovite	350 ± 50 Cº	Jäger et al. (1967)
Biotite	300 ± 50 Cº 350-400 Cº 280-345 Cº	Dodson (1969) Berger and York (1981) Harrison et al. (1985)
K-feldspar	from 350 Cº to 110 Cº	Foland (1974); Harrison (1981) Harrison and McDougall (1982) Lovera et al. (1989) Purdy and Jäger (1976)

Table 2: A few closure temperatures from the literature

Step heating method: The nuclear reaction of potassium to argon activated by the irradiation, it is possible to liberate argon fractions by fusing the sample by temperature steps. Gas fractions are collected and ages measured at each step. For one sample, several ages can therefore be obtained. Plateau portions of the age spectra are defined as comprising at least three contiguous increments, with similar ages (ie. ages that are within 2σ of the mean age). In addition, this plateau should contain a significant proportion of the total ^{39}Ar released (MacDougall, 1999).

Sample preparation and procedure: Samples are reduced in a jaw crusher and through a pulverizer into a coarse powder. This powder is sieved. Mineral separates of biotite, muscovite and K-feldspar were prepared at the University of the Witwatersrand. The separates were purified at the ANU, using conventional magnetic separation and heavy liquid techniques. Separates were wrapped in aluminium packets and placed in a nuclear reactor, along with a standard sample, during 504 hours. After irradiation, the samples were removed from their packaging and 0.3 – 1.0 mg was loaded into tin foil packets for analysis. The samples were individually dropped into a furnace and heated to progressively higher temperatures, with temperatures maintained for fifteen minutes per step. $^{40}Ar/^{39}Ar$ step-heating analyses were carried out on a VG MM 12 mass spectrometer using an electron multiplier detector. Mass discrimination was monitored by analyses of standard air volumes. K/Ca ratios were determined from the ANU laboratory hornblende standard 77-600. The reported data have been corrected for system blanks, mass discrimination, reactor interferences, fluence gradients and atmospheric contamination. Errors associated with the age determinations are 1σ uncertainties and exclude errors in the J-value estimates. The error on the J-value is ± 0.35 %, excluding the uncertainty in the age of GA (which is ~ 1%). Decay constants are those of Steiger and Jager (1977).

c. Data presentation

The step heating technique provided several ages for several individual samples, each of which can be reported in an age spectrum. In such a diagram (Figure 6), the age of each step is plotted versus the fraction of argon released. Age spectra of samples with undisturbed Ar-Ar systems are expected to show constant and uniform apparent ages to form a plateau age (Figure 6). Very often this is not the case, due to variety of reasons; simple and complex spectra are interpreted for individual samples in subsequent chapters.

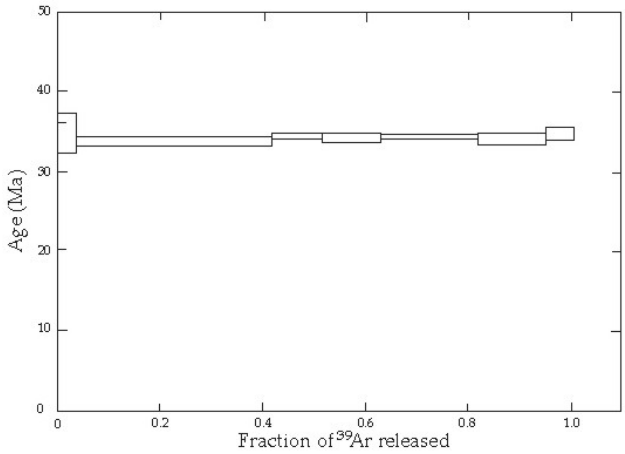

Figure 6: Age spectrum diagram, after York (1984)

5. References

Berger, G. and York, D., 1981. Geochronometry from ^{40}Ar-^{39}Ar dating experiment. Geochimica et Cosmochimica Acta, 45, 795-811.

Compston, W., Williams, I S., Clement, S. W., 1982. U-Pb ages within single zircons using a sensitive high mass-resolution ion microprobe. American Society for Mass Spectrometry Conference 30th, Honolulu, 593-595.

Compston, W., Williams, I. S., Meyer, C., 1984. U-Pb geochronology of zircons from lunar breccia 73217 using a Sensitive High Mass-Resolution Ion Microprobe. Journal of Geophysical Research, 89, B525-B534.

Compston, W., Williams, I. S., Kirschvink, J. L., Zhang, Z., Ma, G., 1992. Zircon U-Pb ages for the Early Cambrian time scale. Journal of the Geological Society, London, 149, 171-184.

Dodson, M. H., 1973. Closure temperature in cooling geochronological and petrological systems. Contributions to Mineralogy and Petrology, 40, 259-274.

Faure, G., 1986. Principles of Isotope Geology, Wiley & Sons, New York, 589 pp.

Foland, K. A., 1974. ^{40}Ar diffusion in homogeneous orthoclase and an interpretation of Ar diffusion in K-feldspar. Geochimica and Cosmoschimica Acta, 38, 151-166.

Harrison, T. M., McDougall, I., 1982. The thermal significance of potassium feldspar K-Ar ages inferred from $^{40}Ar/^{39}Ar$ age spectrum results. Geochimica et Cosmochimica Acta, 46, 1811-1820.

Harrison, T. M., Duncan, I., MacDougall, I., 1985. Diffusion of ^{40}Ar in biotite: Temperature, pressure and compositional effects. Geochimica et Cosmochimica Acta, 49, 2461-2468.

Hayward, C. L., 1998. Cathodoluminescence of ore and gangue minerals and its application in the mineral industry. In: Modern approaches to ore and environment mineralogy, Mineralogical Association of Canada, Ottawa, 27, 269-325.

Jäger, E., Niggli, E., Wenk, E., 1967. Rb-Sr altersbestimmungen and Glimmen der zentralpien. Beitrager zurgol. Karte der Schweiz, NF134, Lieferungen, Kummerly and Frey, Bern.

Lovera, O. M., Richter, F. M., Harrison, T. M., 1989. The $^{40}Ar/^{39}Ar$ thermochronometry for slowly cooled samples having a distribustion of diffusion domain sizes. Journal of Geophysical Research, 94B, 17917-17939.

MacDougall, I., Harrison, T. M., 1999. Geochronology and thermochronology by the ^{40}Ar-^{39}Ar method. Second Edition, Oxford University Press, New York, 269 pp.

Merrihue, C., 1965. Trace element determinations and K-Ar dating by mass-spectrometry of neutron irradiated samples. Transactions – American geophysical Union, Abstract, 46, 126.

Merrihue, C., Turner, G., 1966. Potassium –Argon dating by activation with fast neutrons. Journal of Geophysical Research, 71, 2852-2857.

Mitchell, J. G., 1968. The 40Ar-39Ar method for potassium argon age determination. Geochimica and Cosmochimica Acta, 32, 781-790.

Ourdy, J. W., Jäger, E., 1976. K-Ar ages on rock-forming minerals from the Central Alps. Memoirs, Institute of Geology and Mneralogy, University of Padova, 30, 1-31.

Stacey, J. S., Kramers, J. D., 1975. Approximation of terrestrial lead isotope evolution by a two-stage model. Earth and Planetary Scienc Letters, 26, 207-221.

Steiger, R. H., Jäger, E., 1977. Subcommission on geochronology: convention on the use of decay constants in geo- and cosmochronology. Earth and Planetary Science Letters, 36, 359-362.

Tera, F., Wasserburg, G. J., 1973. A response to a comment on U-Pb systematics in lunar basalts. Earth and Planetary Science Letters, 19, 213-217.

Wetherill, G. S., 1956. An interpretation of the Rhodesia and Witwatersrand age patterns. Geochimica et Cosmochimica Acta, 9, 290-292.

Williams, I. S., Claesson, S., 1987. Isotopic evidence for the Precambrian provenance and Caledonian metamorphism of high grade paragneisses from the Seve Nappes, Scandinavian Caledonides. Contributions to Mineralogy and Petrology , 97, 205-217.

Williams, I. S., 1998. U-Th-Pb geochronology by ion microprobe. Reviews in Economic Geology, 7, 1-35.

York, D., 1984. Cooling histories from $^{40}Ar/^{39}Ar$ age spectra: implications for Precambrian plate tectonics. Earth and Planetary Science Letters, 12, 383-409.